

Magnetically Regulated Gas Accretion in High-Redshift Galactic Disks

Yuval Birnboim

Harvard-Smithsonian Center for Astrophysics, 60 Garden Street, Cambridge MA, USA

ABSTRACT

Disk galaxies are in hydrostatic equilibrium along their vertical axis. The pressure allowing for this configuration consists of thermal, turbulent, magnetic and cosmic ray components. For the Milky Way (MW) the thermal pressure contributes $\sim 10\%$ of the total pressure near the plane, with this fraction dropping towards higher altitudes. Out of the rest, magnetic fields contribute $\sim 1/3$ of the pressure to distances of ~ 3 kpc above the disk plane. In this letter we attempt to extrapolate these local values to high redshift, rapidly accreting, rapidly star forming disk galaxies and study the effect of the extra pressure sources on the accretion of gas onto the galaxies. In particular, magnetic field tension may convert a smooth cold-flow accretion to clumpy, irregular star formation regions and rates. The infalling gas accumulates on the edge of the magnetic fields, supported by magnetic tension. When the mass of the infalling gas exceeds some threshold mass, its gravitational force cannot be balanced by magnetic tension anymore, and it falls toward the disk's plane, rapidly making stars. Simplified estimations of this threshold mass are consistent with clumpy star formation observed in SINS, UDF, GOODS and GEMS surveys. We discuss the shortcomings of pure hydrodynamic codes in simulating the accretion of cold flows into galaxies, and emphasize the need for magneto-hydrodynamic simulations.

Subject headings: galaxies: high-redshift — galaxies: ISM — galaxies: magnetic fields

1. Introduction

This letter deals with the accretion of the cold flows into disk galaxies at $z = 2 - 4$. These star forming galaxies are expected to have large magnetic field, to a degree that will significantly affect the interaction of the cold flows with the disk. In particular, magnetic tension will cause smooth cold flows to enter the disk in a clumpy manner. We derive analytically the typical masses of these clumps and find that for reasonable parameters of the magnetic fields and the disks, the clump masses are $10^7 - 10^9 M_\odot$ as observed. The introduction also contains observational results regarding magnetic fields in the Milky Way (MW) and nearby galaxies (§ 1.1), and clump clusters and clumpy disk galaxies at redshift $z = 2 - 4$ (§ 1.2). In § 2 we derive a toy model for the magnetic tension of a disk (§ 2.1), typical parameters of filamentary cold flows (§ 2.2), and the predicted clump masses (§ 2.3). The importance of magnetic tension for gas accretion calculations and the conclusions are found in § 3.

1.1. The Pressure of the Milky Way and Nearby Galaxies

The gaseous disk of the MW is highly multiphased and contains molecular gas, neutral gas and ionized gas at various temperatures and densities. Since these components are observed in many wavelengths, and by many instruments, it is difficult to combine the observation into one coherent picture of the interstellar medium (ISM). The vertical structure of the Galaxy is constructed of neutral gas and molecules dominating near the disk’s plane, to neutral gas and ionized gas dominating at vertical heights larger than $z \sim 1\text{kpc}$, with a considerable ionized gas density extending out to $\sim 3\text{kpc}$. A compilation of the various components is available in Ferrière (2001). Using this information, one can compare the vertical gravitational attraction indicated by this column mass as well as stars and dark matter to the force arising from the thermal pressure of the combined gaseous components. It is striking that the thermal pressure at the mid-plane only supports $\sim 10\%$ of the pressure required to support the vertical extent of the disk (Badhwar & Stephens 1977; Dehnen & Binney 1998; Cox 2005). This fraction at mid-plane decreases further at larger radii. The remaining 90 – 100% of the pressure at each altitude arises from a non-thermal pressure sources: turbulent, magnetic and cosmic ray pressures. The relative importance of the three components is comparable, indicating that they are roughly in equipartition (Boulares & Cox 1990; Beck et al. 1996, and reference within.). This is currently a widely accepted hypothesis, which is motivated by the physical expectation that supernova explosions drives turbulence (McKee & Ostriker 1977) which enhances seeded magnetic fields. The magnetic fields act to confine the cosmic rays and effectively set the diffusion rate of cosmic rays out of galaxies.

Magnetic fields are measured by observing Zeeman splitting of 21cm, Faraday rotation of linearly polarised radio emitters and radio synchrotron emission of cosmic rays reacting to the magnetic fields. Radio loud nearby disk galaxies such as M51, M83 and NGC6946, have total field strengths of $20 - 30\mu\text{G}$ in their spiral arms (Beck 2009, and reference within.) Bell (2003) showed that the radio emission, most of which is non-thermal synchrotron radiation, which arises from a rough equilibrium between cosmic rays and magnetic fields, correlates with SFR over 5 orders of magnitude in radio emission. The relation $B \sim \text{SFR}^{0.5}$ is expected, and indeed observed, for star-forming galaxies (Lisenfeld, Voelk, & Xu 1996). We do not attempt to model this relation explicitly for our high- z star-forming ($\gtrsim 100M_{\odot} \text{ yr}^{-1}$) galaxies, but adopt, as a lower bound, magnetic field amplitudes of $20 - 100\mu\text{G}$ as reasonable, conservative, extrapolation. A good review of the measurements and typical values of magnetic fields can be found in Beck (2009).

The magnetic field of the MW, a low SFR, radio quiet galaxy, ranges from $6\mu\text{G}$ at the solar neighborhood, to $10\mu\text{G}$ in the inner Galaxy. At the spirals near the center, the magnetic fields can reach $100\mu\text{G}$. While the large scale structure of the MW’s magnetic fields is hard to measure, the Galaxy provides a good probe of small scale magnetic fields. Magnetic fields seem to be entangled between the multiphase components of the ISM on parsec scales. 60% of the field’s strength tends to be in coherent, ordered magnetic structures, correlating on kpc scales with the spiral structures of the MW. At higher altitudes the magnetic field drops, and at 3 kpc it is a factor of 2 lower when fitting synchrotron radiation, and five times lower assuming equipartition (Cox 2005).

It is worthwhile to emphasize the physical situation that arises from these conditions: the magnetic fields are pressurized but do not interact gravitationally. The field would disperse to infinity unless there is a small amount of gas locked between the entangled magnetic field, pulling it towards the disk. While the gas does not contribute a significant amount of thermal pressure, it contributes all the gravitational force, pulling everything together.

1.2. Clumpy Star Formation at High Redshift

During the past few years data have begun to accumulate regarding the structure of high redshift spiral galaxies. Their morphology was investigated using the Hubble Deep Field survey Cowie, Hu, & Songaila (1995) and the Ultra Deep Field (Elmegreen et al. 2005, 2007). They showed that the majority of high- z galaxies are disks, with clumpy, irregular morphology (“Clump clusters” or “Chain galaxies”) and high velocity dispersions. Most of the star formation is observed to be concentrated in a few, well defined clumps with spatial extent of ~ 1 kpc and mass of $10^7 - 10^9 M_\odot$. The inferred velocity dispersion of these galaxies is $20 - 50$ km sec^{-1} . These observations are complemented spectroscopically by observations by the SINS survey (Genzel et al. 2006; Förster Schreiber et al. 2006) that contains 80 H_α emitting galaxies with masses $M \sim 3 \times 10^{10} M_\odot$, most exhibiting rotating irregular gas patterns (Shapiro et al. 2008). Lower redshift information, derived from the GOODS and GEMS surveys, is analyzed in Elmegreen et al. (2009) and from the MASSIV survey in Epinat et al. (2009). Elmegreen et al. (2009) demonstrated that there is an evolutionary sequence of galaxies with the highly irregular clumpy ones at one end (making 50% of the galaxies at $z \sim 4$), and a smoother disk at the other (making 90% of the galaxies at $z \sim 1$).

While these galaxies are star-bursting, with typical SFR of $100 - 200 M_\odot \text{ yr}^{-1}$, most show no signatures of galaxy mergers and appear to maintain their disk. Their gas supply is most likely a result of gaseous cold flows accreting efficiently onto the galaxies (Dekel et al. 2009b; Bournaud & Elmegreen 2009). Gas that is accreted onto the halo is unable to sustain a virial shock because the “would-be” post-shock gas would be cooling faster than it is contracting - unable to provide pressure support for the virial shock. This has been shown analytically by Birnboim & Dekel (2003); Dekel & Birnboim (2006) and numerically by Kereš et al. (2005); Ocvirk, Pichon, & Teyssier (2008); Kereš et al. (2009); Brooks et al. (2009); Agertz, Teyssier, & Moore (2009). There is a broad transition (Dekel & Birnboim 2006; Kereš et al. 2009) between cold-dominated halos and hot-dominated halos at which the accretion is in narrow, cold filaments penetrating through a hot, diffuse halo. The cold flows ($\sim 10^4 K$ gas) flow undisturbed, preferentially perpendicular to the disk’s plane (Dekel et al. 2009b), until the vicinity of the disk. These filaments then deposit their kinetic energy near the disk¹, join the disk and efficiently form stars. Based on lambda cold dark matter (Λ CDM)

¹The slowdown can be gradual, by a series of weak shocks (Kereš et al. (2009); Agertz et al. (2009) using SPH and AMR simulations) or abrupt in a strong, “isothermal” shock (Dekel et al. (2009b); Ocvirk et al. (2008), AMR simulations)

hierarchical formation models Neistein & Dekel (2008); Dekel et al. (2009b) find that 2/3 of the accreted gas are in the form of smooth, cold, inflowing filaments.

Recent theoretical work attempts to show how such clumps can be created. By using hydrodynamic simulations of disks, Bournaud, Elmegreen, & Elmegreen (2007) demonstrated that gas rich disks corresponding to these high- z galaxies break rapidly into clumps via gravitational instability, and that these clumps migrate towards the center, creating a bulge. Dekel, Sari, & Ceverino (2009a) showed that when there is a constant supply of smoothly accreted gas, the disk is maintained marginally Toomre stable, allowing for a prolonged evolution of bulge and clumpy disk consistent with observations. Using high resolution AMR simulations, Agertz et al. (2009) found that clumps naturally form within the disk from cold flows, and that the cold flows do not exhibit strong shocks at the edge of the disks.

2. Disk Accretion in the presence of Magnetic Tension

2.1. Magnetic Tension

In this section we estimate the dynamic effect of magnetic tension on the accretion efficiency of cold-filament gas onto the galaxies. If one pulls a magnetic tube along its field lines, the amplitude of the magnetic field does not change, while the volume it occupies grows. The work required to extend the tube by a distance dl is: $\frac{B^2}{8\pi}Adl$ with A being the surface crosssection of the tube. The tension of the magnetic field is thus:

$$\sigma = \frac{B^2}{8\pi}. \quad (1)$$

The magnetic fields are entangled on some scale, which creates a net of magnetic fields woven through the gas. While the field adjusts quickly to pressure variations, it does react against being bent. The toy model proposed here treats the field as a sheet of elastic matter, being bent inwards by gas that is accreted onto it. As gas falls on top of the magnetic sheet, it will flow and settle at the lowest altitude it can, to minimize its potential energy. We assume that the deflection of the sheet is cylindrically symmetric around the center of the perturbation, and that the magnetic fields are pinned to their initial altitude at some radius by the joint forces of the entangled magnetic fields. We denote the radial direction by r and the vertical dimension by z . The magnetic fields are pinned to z_{\max} at r_{\max} (fig. 1). We solve for the shape of the line $z(r)$ for which the system is static in the presence of mass M_{cl} of gas with density ρ_{gas} . The gas will fill the well in the magnetic fields from the lowest z possible to some height z_{gas} according to:

$$M_{\text{cl}} = \int_0^{r(z_{\text{gas}})} 2\pi r \rho_{\text{gas}}(z_{\text{gas}} - z(r)) dr. \quad (2)$$

The force on some ring element of gas between $[r : r + \Delta r]$ is the sum of the gravitation on that element, and the difference between the vertical component of the tension at $r + \Delta r$ and r :

$$2\pi r(z_{\text{gas}} - z(r))\rho_{\text{gas}}g(z) dr = \quad (3)$$

$$2\pi(r + \Delta r)W\sigma\sin[\theta(r + \Delta r)] - 2\pi rW\sigma\sin[\theta(r)],$$

with $g(z)$ being the gravitational acceleration caused by the disk², $\theta(r)$ the angle between the direction of the line and the horizontal direction, and W the width of the elastic layer (see fig. 1). Throughout this work we assume that the width of the magnetic layer being bent scales like the amplitude of the perturbation, up to a factor l_W :

$$W = l_W \times (z_{\max} - z(0)). \quad (4)$$

A more sophisticated decision would require observational data or MHD calculations about the shape of the magnetic fields. The solution of eq. 2 and 3 is found by integrating from 0 to r_{\max} with $[z_{\text{gas}}, z(0)]$ as boundary conditions, and fitting them to find the required values of $[M_{\text{cl}}, z(r_{\max})]$. by the simplex numerical method (Press et al. 1996).

2.2. Magnetically Supported Gaseous Blobs

In an effort to relate this magnetic tension to realistic cosmological conditions some typical parameters are chosen. The following is a rather lengthy “back of the envelope” calculation intended to estimate the density of the infalling gas as it interacts with the magnetic field. The puncture mass, actually, does not strongly depend on this density, but it is of deductive value to work out these numbers non-the-less. Based on simulations we assume 3 conical filaments, each at roughly $2\Theta = 20^\circ$ in diameter. The temperature of the filaments is $T_{\text{fil}} = 2 \times 10^4 K$ and they are in hydrostatic equilibrium with the virialized hot gas which is at T_{vir} . The density of the filaments in these conditions is $\rho_{\text{fil}} = f_b \rho_u \delta_{\text{OD}} [(T_{\text{fil}}/T_{\text{vir}})(1 - 3\pi\Theta^2/4\pi) + 3\Theta^2/4]^{-1}$, with f_b, ρ_u and δ_{OD} being the universal baryonic fraction, density and virial overdensity respectively. We assume that the velocity of the filament is roughly the sound speed of the hot component ($c_s^2 = \gamma k_B T_{\text{vir}} N_A / \mu$). The global accretion rate \dot{M} for halo mass M_{vir} at redshift z is taken from Neistein & Dekel (2008); Dekel et al. (2009b) which sets the radius of each of the three filaments near the disk according to: $\dot{M}/3 = \pi R_{\text{fil}}^2 c_s \rho_{\text{fil}}$. Finally, the infalling gas in the filament is stopped, converting its kinetic energy to thermal energy. The strong shock or set of weak shocks would adjust themselves so the ram-pressure of the infalling gas is balanced by the dense, halted gas below. Assuming that the post-shock pressure is all thermal the filament density at the edge of the disk is $\rho_{\text{edge}} = \rho_{\text{fil}} c_s^2 / (k_B T_{\text{fil}} N_A \mu^{-1})$. For $M_{\text{halo}} = 10^{12} M_\odot, z = 2$ we have: $\rho_{\text{edge}} = 8 \times 10^{-24} \text{gr cm}^{-3}, c_s =$

²throughout this work we use a fit for the vertical gravitational profile from Cox (2005) that takes into account the gas components, as well as the star and dark matter contribution. For different disk column densities the gravitational force is scaled, but its shape and z-dependence is not changed. The observed values of column densities by Elmegreen et al. (2009) of $z \sim 2 - 4$ galaxies ($\sim 100 M_\odot \text{pc}^{-2}$) are roughly the same as those of the MW. Since σ and g in eq. 3 are proportional, a change in the scaling of the gravitation corresponds to a change in the square of the magnetic fields.

180km sec⁻¹, $\dot{M} = 78M_{\odot} \text{ yr}^{-1}$, $R_{\text{fil}} = 7\text{kpc}$ and for $z = 4$ we have: $\rho_{\text{edge}} = 7 \times 10^{-23}\text{gr cm}^{-3}$, $c_s = 230\text{km sec}^{-1}$, $\dot{M} = 250M_{\odot} \text{ yr}^{-1}$ and $R_{\text{fil}} = 4\text{kpc}$.

The final densities at the edge of the disks are upper limits. If some of the pressure of this gas is in turbulent form, or if the energy carried by the filament is spread over a larger volume, this density would be lower. It can be easily shown that the gas at the edge of the disk is in rough pressure equilibrium with the total pressure of the disk as is the case for the MW. However, while the MW’s density is smooth and monotonically decreasing as z increases, no monotonic density profile is possible for cold accretion. When the temperature above the disk is similar to that of the disk, the extra pressure terms at the disk require that the density above the disk be larger than at the disk. This gas would sink in (via Rayleigh Taylor instabilities) unless the disk has surface tension such as the magnetic tension discussed here. The ionization fraction of the infalling gas is also of interest because the magnetic fields interact only with ionized gas. We expect that gas at $1 - 2 \times 10^4 K$ and densities as mentioned above the gas will always be sufficiently ionized so that ambipolar diffusion will be ineffective³.

2.3. Typical Masses of Magnetic Tension Induced Clumps

The mass of clump for which the clump can puncture through the magnetic tension depends on the magnetic strength (eq. 3), width of the sheared layer (eq. 4; $l_W = 0.3$. throughout this section) , the gravitational profile of the disk, the density (through eq. 2 and 3) and on the radius at which magnetic fields are assumed to be pinned to their location by the global forces of the disk ($R_{\text{max}} = 3\text{kpc}$ throughout this section). Figure 2 shows four clump masses at density $10^{-23}\text{gr cm}^{-3}$ and magnetic field of $100\mu G$. As the mass increases, the gravitation bends the magnetic fields and gas fills the lowest potential energy possible. The puncture mass is just above $M_{\text{cl}} = 10^9 M_{\odot}$.

Figure 3 shows the puncture mass for various gas densities and magnetic fields. For the MW, the magnetic tension will not affect the accretion of gas onto the galaxy (the “MW” rectangle in the figure). However, for larger magnetic fields and reasonable gas densities (marked with the “high- z ” rectangle in fig. 3) the mass of clumps that can penetrate is determined by the magnetic tension. For a wide range of parameters, particularly for high magnetic fields and lower accretion densities, the puncture mass increases to $\gtrsim 10^{10} M_{\odot}$. This gas will break through the magnetic fields instantaneously, yielding large gas fractions which are necessary for the in-situ clump instabilities found in Bournaud & Elmegreen (2009). The degree of coherence of ages of stars in the clumps is a good test for this scenario.

³The timescale for ambipolar diffusion of neutral gas with number density and ionization fraction of $n = 1 \text{ cm}^{-3}$, $x = 10^{-3}$ through magnetic fields $B \sim 20\mu G$ over a distance of $\sim 1 \text{ kpc}$ is $t > 10^{11} \text{ yr}$ (Brandenburg & Zweibel 1994).

3. Discussion

We have shown that for $z = 2 - 4$ star forming galaxies the magnetic fields at the edge of the disk are strong enough to alter the behavior of gas falling onto these disks. The expected magnetic tension is capable of stopping the cold accretion until some threshold mass is accumulated, at which point the clump punctures through the magnetic fields and falls into the disk. The model could either produce individual clumps, or suppress accretion onto the galaxy for long periods of times, causing critical, coherent star-bursts on global galactic scales. Since the estimation of the magnetic field strengths here is very conservative, the magnetic tension will probably also affect gas accretion in more typical star forming galaxies with rates of $\leq 100M_{\odot}\text{yr}^{-1}$. The model depends on the shape, correlation length and strength of the magnetic fields which are poorly known by theoretical considerations and extrapolation from local galaxies. There are no observational constraints on magnetic fields at these redshifts.

For the MW, and nearby quiescent spirals, the magnetic fields are not strong enough to significantly affect the gas accretion, and the SFR will be dominated by the supply rate and other processes. Even if the magnetic fields were stronger, the time that would take for significant clumps to accumulate (at $1 - 4M_{\odot}\text{yr}^{-1}$) would be long with respect to the time it takes for magnetic fields to realign, which should be of the order of the dynamical time of the disk. This is not the case when the accretion rate is $\gtrsim 100M_{\odot}\text{yr}^{-1}$.

Neutral gas can potentially flow through the magnetic fields. The conditions required for such a process are typical for molecular clouds with extremely low ionization fractions. The relatively low densities and high temperatures ($T_{\text{gas}} = 2 \times 10^4 K$) discussed here will render this ambipolar diffusion negligible.

The toy model described in § 2 should not be taken at face value. It should, however, serve as an indication that non-thermal pressure components will have a significant, non-trivial dynamic effect on the accretion of gas onto galaxies. Pure hydrodynamic simulations are missing the effects of magnetic fields and cosmic rays, which account for $\sim 2/3$ of the pressure in the disk. This could be compensated in part by a correct choice of the cooling function or the equation of states of star forming regions (Springel & Hernquist 2003). However, no form of gaseous equation of state can produce stress-strain behavior similar to that of magnetic tension. If this is important, full MHD codes should be used. Hydrodynamic simulations will predict correctly the shape and mass of the gaseous halo, the rate of the infalling gas and the cold filaments. They will also predict correctly the overall SFR of galaxies, because it is basically a question of gas supply. They are not expected to correctly predict the local, or temporal gas accretion or SFR, when the accretion is faster than typical mixing times in the disk. Other processes, such as angular momentum transfer in the disk, will depend on the dynamics within the disk which are dominated by non-thermal pressure. Shocks and sound waves in the disk will depend on the turbulence and Alfvén speeds, rather than on the sound speed of the gas.

I thank Donald Cox for spending time and effort to walk me through the magnetic field

calculations, and Shmulik Balberg for useful discussions and good advice. I thank the referee, Frederic Bournaud for useful comments.

REFERENCES

- Agertz, O., Teyssier, R., & Moore, B. 2009, MNRAS, 397, L64
- Badhwar, G. D., & Stephens, S. A. 1977, ApJ, 212, 494
- Beck, R. 2009, IAU Symposium, 259, 3
- Beck, R., Brandenburg, A., Moss, D., Shukurov, A., & Sokoloff, D. 1996, ARA&A, 34, 155
- Bell, E. F. 2003, ApJ, 586, 794
- Birnboim, Y., & Dekel, A. 2003, MNRAS, 345, 349
- Boulares, A., & Cox, D. P. 1990, ApJ, 365, 544
- Bournaud, F., & Elmegreen, B. G. 2009, ApJ, 694, L158
- Bournaud, F., Elmegreen, B. G., & Elmegreen, D. M. 2007, ApJ, 670, 237
- Brandenburg, A., & Zweibel, E. G. 1994, ApJ, 427, L91
- Brooks, A. M., Governato, F., Quinn, T., Brook, C. B., & Wadsley, J. 2009, ApJ, 694, 396
- Cowie, L. L., Hu, E. M., & Songaila, A. 1995, AJ, 110, 1576
- Cox, D. P. 2005, ARA&A, 43, 337
- Dehnen, W., & Binney, J. 1998, MNRAS, 294, 429
- Dekel, A., & Birnboim, Y. 2006, MNRAS, 368, 2
- Dekel, A., Sari, R., & Ceverino, D. 2009a, ArXiv e-prints
- Dekel, A., et al. 2009b, Nature, 457, 451
- Elmegreen, D. M., Elmegreen, B. G., Marcus, M. T., Shahinyan, K., Yau, A., & Petersen, M. 2009, ApJ, 701, 306
- Elmegreen, D. M., Elmegreen, B. G., Ravindranath, S., & Coe, D. A. 2007, ApJ, 658, 763
- Elmegreen, D. M., Elmegreen, B. G., Rubin, D. S., & Schaffer, M. A. 2005, ApJ, 631, 85
- Epinat, B., et al. 2009, ArXiv e-prints
- Ferrière, K. M. 2001, Reviews of Modern Physics, 73, 1031

- Förster Schreiber, N. M., Genzel, R., Lehnert, M. D., Bouché, N., Verma, A., Erb, D. K., Shapley, A. E., & et al.. 2006, *ApJ*, 645, 1062
- Genzel, R., Tacconi, L. J., Eisenhauer, F., Förster Schreiber, N. M., Cimatti, A., Daddi, E., Bouché, N., & et al.. 2006, *Nature*, 442, 786
- Kereš, D., Katz, N., Davé, R., Fardal, M., & Weinberg, D. H. 2009, *MNRAS*, 396, 2332
- Kereš, D., Katz, N., Weinberg, D. H., & Davé, R. 2005, *MNRAS*, 363, 2
- Lisenfeld, U., Voelk, H. J., & Xu, C. 1996, *A&A*, 314, 745
- McKee, C. F., & Ostriker, J. P. 1977, *ApJ*, 218, 148
- Neistein, E., & Dekel, A. 2008, *MNRAS*, 383, 615
- Ocvirk, P., Pichon, C., & Teyssier, R. 2008, *MNRAS*, 390, 1326
- Press, W. H., Teukolsky, S. A., Vetterling, W. T., & Flannery, B. P. 1996, *Numerical Recipes in Fortran 90* (Cambridge University Press)
- Shapiro, K. L., et al. 2008, *ApJ*, 682, 231
- Springel, V., & Hernquist, L. 2003, *MNRAS*, 339, 289

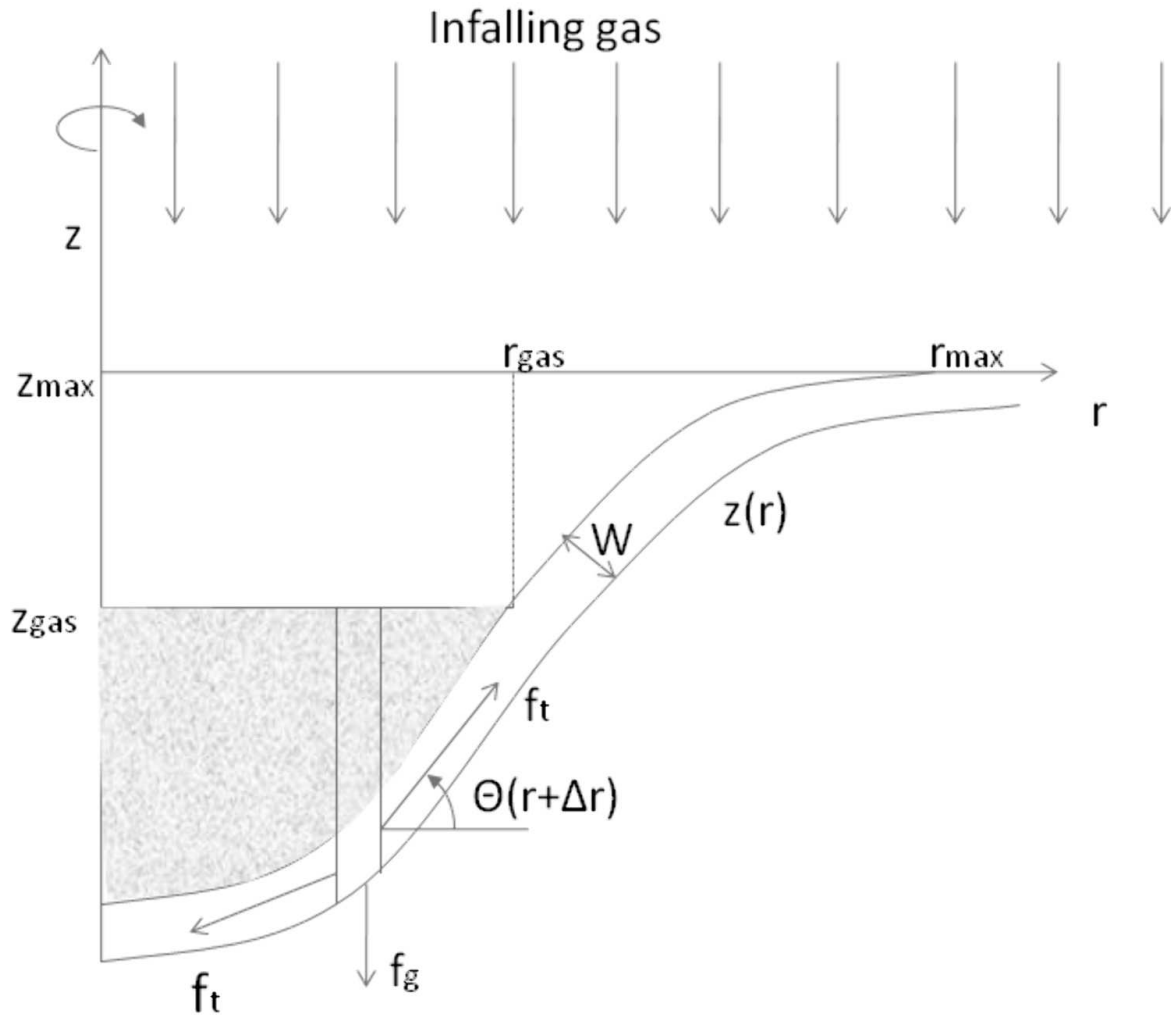


Fig. 1.— A schematic representation of the magnetic tension sheet and the forces acting on it.

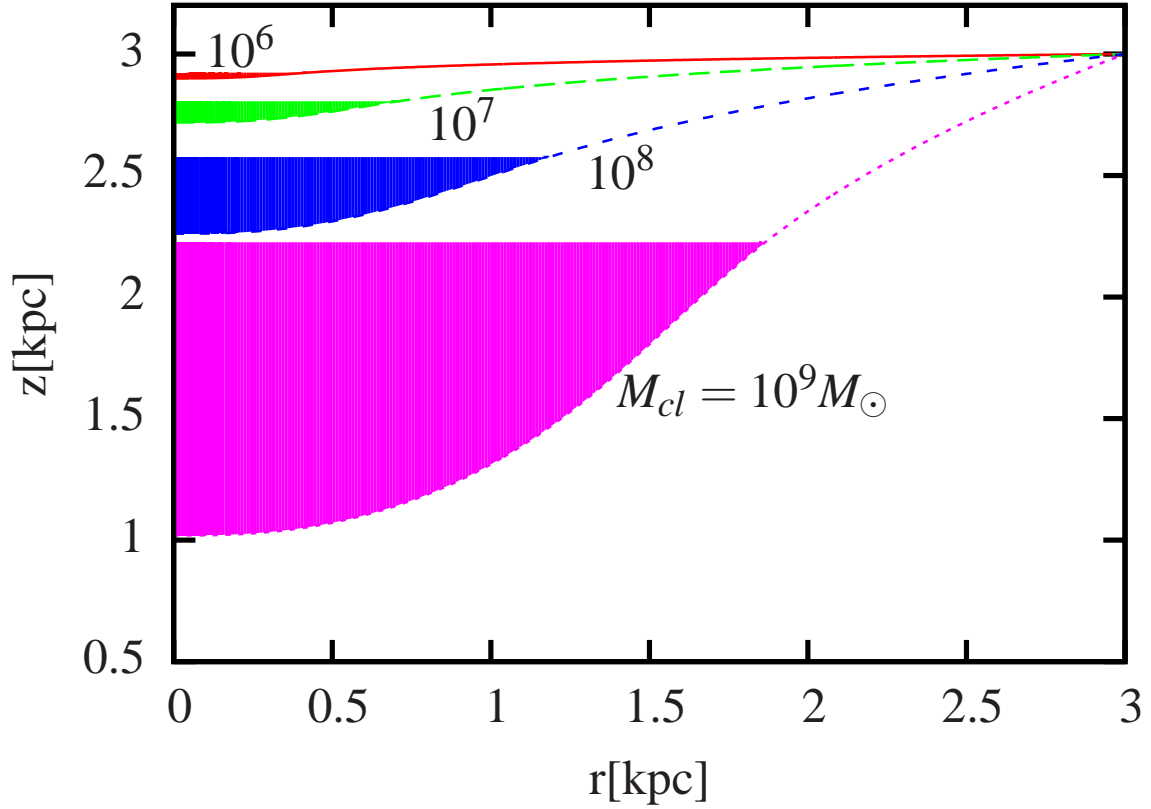


Fig. 2.— The evolution of the magnetic layer as the mass is increased from $10^6 - 10^9 M_{\odot}$. The magnetic fields react to the weight of the gas by bending inwards, until, around $10^9 M_{\odot}$ the tension cannot support the weight any more and a static solution becomes impossible. The gas density, magnetic field, shear layer width and maximal radius of perturbation are $\rho_{\text{gas}} = 10^{-23} \text{gr cm}^{-3}$, $B = 100 \mu\text{G}$, $l_W = 0.3$, $R_{\text{max}} = 3 \text{kpc}$.

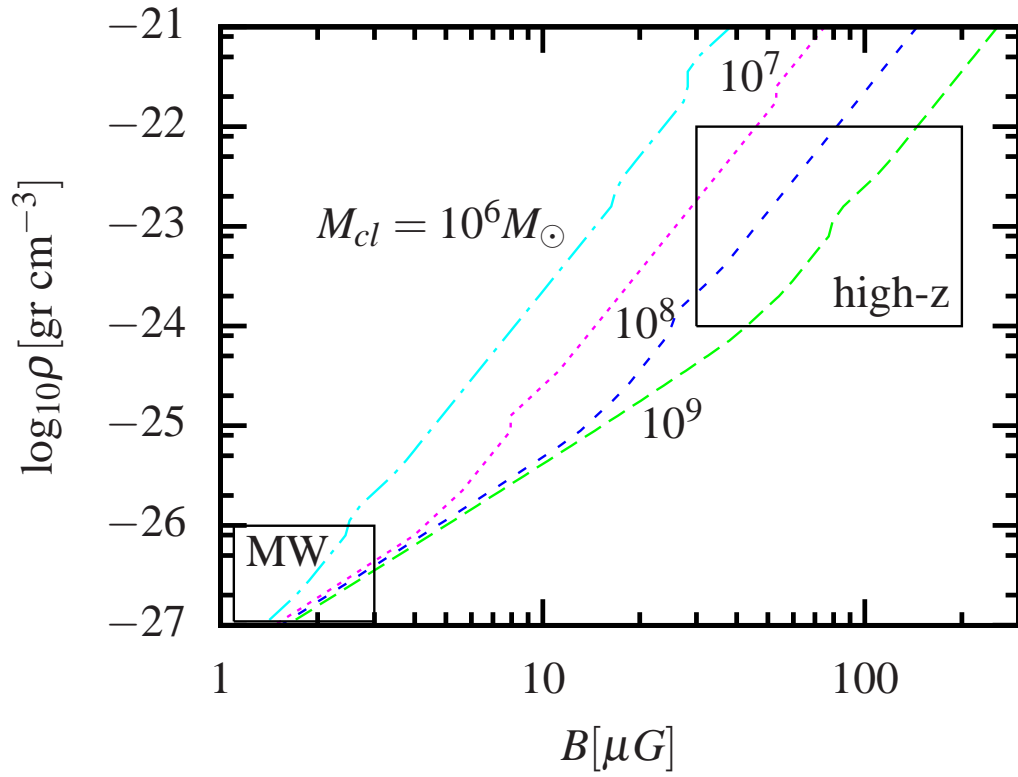


Fig. 3.— The dependence of the puncture mass (various lines) on the magnetic field (x-axis) and density (y-axis). The rectangles mark typical values for the MW and high-z galaxies in that parameter space.